JOURNAL OF TISSUE ENGINEERING AND REGENERATIVE MEDICINE
RESEARCH ARTICLE

Efficacy of thermoresponsive, photocrosslinkable hydrogels derived from decellularized tendon and cartilage extracellular matrix for cartilage tissue engineering

Benjamin B. Rothrauff[1,2†] | Luca Coluccino[1,3,4†] | Riccardo Gottardi[1,5] | Luca Ceseracciu[3] | Silvia Scaglione[4] | Luca Goldoni[3] | Rocky S. Tuan[1,2]

[1]Center for Cellular and Molecular Engineering, Department of Orthopaedic Surgery, University of Pittsburgh, Pittsburgh, PA, USA
[2]McGowan Institute for Regenerative Medicine, University of Pittsburgh, Pittsburgh, PA, USA
[3] Istituto Italiano di Tecnologia, Genoa, Italy
[4] IEIIT Institute, CNR!National Research Council of Italy, Genoa, Italy
[5]Fondazione RiMED, Palermo, Italy

Authors' Accepted Manuscript (AAM): This is the accepted version of the paper
J Tissue Eng Regen Med 2018; 12: e159-e170
Published online 21 August 2017 in Wiley Online Library (wileyonlinelibrary.com)

Efficacy of thermoresponsive, photocrosslinkable hydrogels derived from decellularized tendon and cartilage extracellular matrix for cartilage tissue engineering

Benjamin B. Rothrauff[1,2†] | Luca Coluccino[1,3,4†] | Riccardo Gottardi[1,5] | Luca Ceseracciu[3] | Silvia Scaglione[4] | Luca Goldoni[3] | Rocky S. Tuan[1,2]

Abstract

Tissue engineering using adult mesenchymal stem cells (MSCs), a promising approach for cartilage repair, is highly dependent on the nature of the matrix scaffold. Thermoresponsive, photocrosslinkable hydrogels were fabricated by functionalizing pepsin-soluble decellularized tendon and cartilage extracellular matrices (ECM) with methacrylate groups. Methacrylated gelatin hydrogels served as controls. When seeded with human bone marrow MSCs and cultured in chondrogenic medium, methacrylated ECM hydrogels experienced less cell-mediated contraction, as compared against non-methacrylated ECM hydrogels. However, methacrylation slowed or diminished chondrogenic differentiation of seeded MSCs, as determined through analyses of gene expression, biochemical composition and histology. In particular, methacrylated cartilage hydrogels supported minimaldue to chondrogenesis over 42 weeks, as hydrogel disintegration beginning at day 14 presumably compromised cell–matrix interactions. As compared against methacrylated gelatin hydrogels, MSCs cultured in non-methacrylated ECM hydrogels exhibited comparable expression of chondrogenic genes (Sox9, Aggrecan and collagen type II) but increased collagen type I expression. Non-methacrylated cartilage hydrogels did not promote chondrogenesis to a greater extent than either non-methacrylated or methacrylated tendon hydrogels. Whereas methacrylated gelatin hydrogels supported relatively homogeneous increases in proteoglycan and collagen type II deposition throughout the construct over 42 days, ECM hydrogels possessed greater heterogeneity of staining intensity and construct morphology. These results do not support the utility of pepsin-solubilized cartilage and tendon hydrogels for cartilage tissue engineering over methacrylated gelatin hydrogels. Methacrylation of tendon and cartilage ECM hydrogels permits thermal- and light-induced polymerization but compromises chondrogenic differentiation of seeded MSCs.

KEYWORDS

cartilage tissue engineering, extracellular matrix, hydrogel

1 | INTRODUCTION

Dense connective tissues, such as tendon, ligament, hyaline cartilage and fibrocartilage, possess a poor intrinsic healing capacity that contributes to a high rate of injury and chronic morbidity (Lomas et al., 2015; Makris, Gomoll, Malizos, Hu, & Athanasiou, 2015). Engineered scaffolds composed of synthetic or biological materials have been fabricated in an effort to provide a tissue-specific microenvironment capable of inducing cells to restore the structure and function of the native tissue. Biological scaffolds derived from decellularized tissues have been utilized, given the potential preservation of mechanical, topographical and biochemical cues found in the native tissue (Crapo, Gilbert, & Badylak, 2011). In fact, decellularized tendon (Ning et al., 2015; Yin et al., 2013), cartilage (Sutherland, Converse, Hopkins, & Detamore, 2015) and meniscus (Stabile et al.,2010) have shown promise in promoting tissue-specific

†Authors contributed equally to this study.

(i.e. homologous) phenotypes of seeded cells. However, the dense collagenous extracellular matrix (ECM) that constitutes these tissues presents a challenge for sufficient decellularization and subsequent cellular repopulation, with seeded cells often limited to the superficial regions (Schwarz et al., 2015; Schwarz et al., 2012). The decellularized ECM can be milled into particles in order to increase pore size and facilitate cell infiltration, but these scaffolds require lyophilization in geometrically defined molds with subsequent chemical or thermal crosslinking prior to cell seeding (Cheng Estes, Young, & Guilak, 2013; Rowland, Lennon, Caplan, & Guilak, 2013). This approach produces scaffolds with a limited number of geometric shapes and requires ex vivo cell culture to permit adequate cell attachment and migration, both limiting clinical translation as a point-of-care therapeutic.

On the other hand, enzymatic digestion (most commonly with pepsin) of decellularized ECM results in injectable hydrogels that can fill abnormally shaped defects and are capable of supporting intraoperative cell seeding. These hydrogels undergo thermoresponsive polymerization at body temperature, with tissue sources including, among others, menis-cus (Wu et al., 2015), tendon (Farnebo et al., 2014; Kim et al., 2014) and cartilage (Pati et al., 2014). Although these thermoresponsive hydrogels demonstrate excellent cytocompatibility and biocompatibility when respectively seeded with cells or implanted in vivo, the preservation of biological cues capable of promoting tissue-specific cellular phenotypes remains largely unexplored (Keane et al., 2015). Furthermore, they possess mechanical properties inferior to native tissues and undergo rapid cell-mediated contraction, limiting their utility as load-bearing or space-filling scaffolds (Wolf et al., 2012). Recently, Gaudet and Shreiber (2012) methacrylated native collagen type I fibrils capable of undergoing thermoresponsive self-polymerization with further crosslinking upon exposure to ultraviolet (UV) light. Importantly, neither the methacrylation process nor the photoinducible crosslinking significantly disrupted the architecture of the nanofibrous collagen network formed at 37 °C. Subsequently, Visser, Levett, et al. (2015) added methacrylate functional groups to pepsin-digested decellularized ECM derived from cartilage, meniscus and tendon, which were then added to methacrylated gelatin (GelMA) hydrogels. Supplementation of GelMA with the methacrylated cartilage ECM did not promote chondrogenesis of seeded mesenchymal stem cells (MSCs) to a greater extent than the other ECM sources, yet its inclusion as a supplemental component of GelMA hydrogel may have diluted any tissue-specific bioactivity.

The purposes of this study were: (1) to fabricate methacrylated hydrogels derived from decellularized cartilage and tendon ECM that were capable of undergoing both thermoresponsive gelation and photoinducible crosslinking, and (2) to characterize their ability to promote chondrogenic differentiation of seeded MSCs as compared against GelMA and non-methacrylated ECM hydrogels.

2 | MATERIALS AND METHODS

2.1 | Decellularization of tendon and cartilage ECM

Patella tendons and hyaline cartilage of the femoral condyles were harvested from juvenile (6–8 weeks old) cow hindlimbs (Research 87, Boylston, MA, USA) and stored at −20 °C in a protease inhibitor solution composed of 1× phosphate-buffered saline (PBS, Gibco, Grand Island, NY, USA) supplemented with 5 mM ethylenediaminetetraacetic acid (EDTA; Sigma-Aldrich, St. Louis, MO, USA) and 0.5 mM phenylmethylsulfonyl fluoride (PMSF; Sigma-Aldrich) until use. Tissues were thawed overnight at 4 °C, minced (8–27 mm^3) and cryomilled into a fine powder (Spex Freezer Mill 8670, Metuchen, NJ, USA). Powderized tissue (4 g) was agitated for 24 h at 4 °C in 40 ml protease inhibitor solution containing 1% Triton X-100 (Sigma-Aldrich), followed by three washes (30 min each at 4 °C) in 1× PBS. Subsequently, 40 ml Hanks Buffered Salt Solution (HBSS, Thermo Fisher Scientific, Pittsburgh, PA, USA) supplemented with 200 U/ml DNase and 50 U/ml RNase (Worthington, Lakewood, NJ, USA) was added to the powder, with continuous agitation for 12 h at room temperature. The powder was washed six times in 1× PBS, as above, before freezing and subsequent lyophilization. Native tissues and dried decellularized powder were then evaluated for histological appearance, cellular content and biochemical composition, including total collagen and sulfated glycosaminoglycan (sGAG) content, as described below.

2.2 | Histology of native and decellularized ECM

Native and decellularized tissues were fixed in 10% phosphate-buffered formalin, serially dehydrated, embedded in paraffin and then sectioned (6 μm thickness) with a microtome (Leica RM2255, Leica Biosystems, Buffalo Grove, IL, USA). Samples were rehydrated and stained with haematoxylin & eosin (H&E, Sigma-Aldrich) or 4',6-diamidino-2-phenylindole, dilactate (DAPI, Life Technologies, Carlsbad, CA, USA). H&E-stained samples were photographed using an Olympus SZX16 stereo microscope, whereas DAPI-stained sections were visualized with an Olympus CKX41 inverted microscope using fluorescent excitation at 405 nm.

2.3 | Biochemical composition of decellularized ECM

To determine the biochemical composition of native and decellularized tissues, dry samples were digested overnight at 65 °C at a concentration of 10 mg/ml in a digestion buffer (pH 6.0) containing 2% papain (v/v, from Papaya latex, Sigma-Aldrich), 0.1 M sodium acetate, 0.01 M cysteine HCl and 0.05 M EDTA. Concentrated NaOH was subsequently added to the digestion solution to adjust the pH to 7.0. sGAG content was quantified with a Blyscan Assay according to the manufacturer's instructions (Biocolor, Carrickfergus, UK). Double-stranded (dsDNA) content was determined using the Quant-iT Picogreen dsDNA assay (Life Technologies). Total collagen was of determined using a modified hydroxyproline assay. Briefly, 200 μl each sample was hydrolyzed with an equal volume of 4 N NaOH at 121 °C for 75 min, neutralized with an equal volume of 4 N HCl and then titrated to an approximate pH of 7.0. The resulting solution was combined with 1.2 ml chloramine-T (14.1 g/l) in buffer (50 g/l citric acid, 120 g/l sodium acetate trihydrate, 34 g/l NaOH and 12.5 g/l acetic acid) and allowed to stand at room temperature for 30 min. The solution was then combined with 1.2 ml 1.17 mM p-dimethylaminobenzaldehyde in perchloric acid and placed in a 65 °C water bath for 20 min. Each sample (200 μl) was added to a clear

96-well plate, in duplicate, and absorbance at 550 nm was read. PureCol bovine collagen (3.2 mg/ml; Advanced Biomatrix, Carlsbad, CA, USA) was serially diluted to provide a standard curve ranging from 0 to 1000 μg/ml.

2.4 | Preparation of GelMA

GelMA was synthesized by adapting a previously established protocol (Lin, Cheng, Alexander, Beck, & Tuan, 2014). Briefly, 15 g gelatin (Type A, from porcine skin, Sigma-Aldrich) was dissolved in 500 ml deionized H_2O at 40 °C and then 15 ml methacrylic anhydride (Sigma-Aldrich) was added dropwise under vigorous stirring. The mixture was placed at 37 °C in an orbital shaker at 150 rpm for 24 h. The resulting GelMA was dialyzed for 4 days against H_2O at room temperature using 2000 NMWCO dialysis tubing (Sigma-Aldrich) to completely remove alllow molecular weight by-products, with changes in H_2O twice daily. After lyophilization, the product was stored at –20 °C until future use. Prior to use, GelMA was reconstituted at 10% (w/v) in HBSS. Visible light-sensitive photoinitiator lithium phenyl-2,4,6-trimethylbenzoylphosphinate (LAP; 0.25% v/v) was then dissolved by gentle shaking at room temperature. Photocrosslinking was induced by exposure to UV light (LED bulbs, 390–395 nm, 0.5 W) for 2 min.

2.5 | Preparation of ECM hydrogels

To form thermoresponsive (i.e. non-methacrylated) hydrogels, decellularized tendon and cartilage ECM powders were enzymatically digested in a solution of 1 mg/ml porcine pepsin (Sigma-Aldrich) in 0.01 N HCl for 48 h at room temperature under continuous stirring. To induce gelation, digested tendon and cartilage ECM were neutralized by the addition of one-tenth digest volume of 0.1 N NaOH and one-ninth digest volume of 10× PBS, then warmed to 37 °C for 1 h, as reported previously (Keane et al., 2015; Wolf et al., 2012). The stock concentration of tendon and cartilage ECM hydrogels was 30 mg/ml.

To form thermoresponsive, photocrosslinkable (i.e. methacrylated) hydrogels, decellularized tendon and cartilage ECM were pepsin-solubilized as described above. The pH was increased to 7.5 before adding methacrylic anhydride dropwise (3% w/v) under continuous stirring at 4 °C for 12 h. The final product was dialyzed against deionized H_2O for 3 days with changes in water occurring twice daily. After freezing and lyophilization, the methacrylated ECM powder could be reconstituted into a hydrogel by employing the same protocol as for the non-methacrylated hydrogels. After 48 h of pepsin solubilization, 0.25% v/v LAP was added at 4 °C. As with non-methacrylated ECM hydrogels, the methacrylated hydrogel solutions were pH and salt balanced. Temperature-mediated gelation was initiated by incubation at 37 °C for 1 h. Photocrosslinking could be induced by exposure to UV light for 2 min.

2.6 | NMR analysis

^1H NMR was used both to confirm derivatization with the methacrylate group and to calculate the degree of functionalization (DOF). The NMR experiment was performed on a Bruker AvanceIII 600 MHz spectrometer equipped with 5 mm QCI cryoprobe with z shielded pulsed-field gradient coil. In the (1D)-NOESY presat.experiment, 512 transients were accumulated, at a fixed receiver gain, using 65536 complex data points (AQ time 2.73 s) over a spectral width of 20.0 ppm, with a relaxation delay of 30 s and a power level of 1.5697^{-5} W for the water suppression. Before each acquisition, automatic matching and tuning were run, the 90° pulse was optimized by an automatic pulse calculation routine and the homogeneity automatically adjusted. Before data acquisition the sample was equilibrated for 2 min inside the probe and the temperature was actively controlled at 303 K. The spectrum was manually phased and automatically baseline corrected.No slope and bias correction was used for the peak integration. Methacrylated cartilage (CartilageMA) was reconstituted at 1% w/v in 0.1 M D_2O/DCl with 1 mg/ml pepsin. Multiplicity edited heteronuclear single quantum coherence (edited ^1H-^{13}C HSQC) was performed as follows: 64 FIDs, 2048 data points, 256 increments, $^1J_{CH}$ = 145 Hz, spectral width of 7.79 ppm for ^1H and 165.6 ppm for ^{13}C (transmitter frequency offsets at 4.0 and 74.6 ppm, respectively).

2.7 | Surface ultrastructure

All hydrogels were examined by scanning electron microscopy (SEM) at different stages of crosslinking. Namely, hydrogels were collected after the following steps: (1) at 4 °C, before UV light exposure; (2) at 4 °C, followed by 2 min of UV light exposure; (3) at 37 °C, before UV light exposure and (4) at 37 °C, followed by UV light exposure. At each stage, hydrogels were fixed at 4 °C in 2.5% (v/v) glutaraldehyde (Electron Microscopy Sciences,Hatfield, PA, USA) in 1× PBS for 3 h under gentle shaking. Hydrogels were washed three times in 1× PBS (20 min/wash) then dehydrated in a series of increasing ethanol concentrations (25%, 50%, 75%, 95%, 100%, 100%, 1 h/concentration) at 4 °C. Dehydrated hydrogels were stored in 100% ethanol at 4 °C until critical point drying (LeicaEM CPD030 Critical Point Dryer, Leica Biosystems).Once dry, hydrogels were sputter-coated with 4.5 nm gold and imaged by SEM (field emission, JEOL JSM6335F, Peabody, MA, USA) operated at 3 kV accelerating voltage and 8 mm working distance.

2.8 | Isolation of human MSCs

Human MSCs were obtained as previously described (Lin, Yang, Tan, & Tuan, 2012). Briefly, human bone marrow was obtained from femoral heads of patients undergoing total hip arthroplasty with institutional review board approval (University of Washington and University of Pittsburgh). Trabecular bone was cored out using a curette or rongeur and flushed with rinsing medium (αMEM, 1% Anti-Anti, Life Technologies) using 18G hypodermic needles. The marrow flushed from minced bone chips was passed through 40 μm mesh screens to remove debris and cells were pelleted by centrifugation for 5 min at 300×g. After rinsing, cells were resuspended in MSC growth medium [αMEM, 10% fetal bovine serum (Life Technologies), 1% Anti-Anti and 1 ng/ml FGF-2 (Peprotech,Rocky Hill, NJ, USA)] and then plated into 150 cm^2 tissue culture flasks. On day 4, cells were washed with PBS and fresh growth medium was added.The medium was changed every 3 days. Once 80% confluence was reached, cells were detached with 0.25% trypsin containing 1 m M EDTA (Life Technologies) and

passaged. MSC populations isolated from individual patients were routinely validated as capable of osteogenic, adipogenic and chondrogenic differentiation (data not shown). All experiments were performed with passage 3 MSCs. MSCs from three patients (31-year-old female, 42-year-old male, 44-year-old male) were pooled for this study.

2.9 | In vitro cell culture

MSCs were homogenously suspended in one of five hydrogels: (1) GelMA, (2) non-methacrylated tendon (tendon), (3) non-methacrylated cartilage (cartilage), (4) methacrylated tendon (TendonMA) or (5) CartilageMA at a concentration of 20×10^6 cells/ml. Before gelation, MSC-seeded hydrogels (~50 µl) were distributed at 4 °C to silicone moulds measuring 5 mm diameter × 2 mm depth. To induce thermal gelation, hydrogels were placed in an incubator at 37 °C for 1 h. Thereafter, all hydrogel groups were exposed to 2 min of UV light to induce crosslinking between unreacted methacrylate groups, when present. MSC-seeded hydrogels were then removed from silicone moulds and transferred to six-well plates previously coated with silicone (Sigmacote, Sigma-Aldrich) to prevent cell migration and adhesion on to the plastic surface. Constructs were cultured up to 42 days in chondrogenic medium [DMEM, 1% Anti-Anti, 10 µg/ml insulin, transferrin, selenium (ITS+), 0.1 µM dexamethasone, 40 µg/ml proline, 50 µg/ml ascorbate-2-phopshate, 10 ng/ml transforming growth factor β3 (TGF-β3, Peprotech)].

2.10 | Cell-mediated contraction of hydrogels

The surface area of cylindrical constructs was measured on days 0, 7, 14, 21 and 42 using an Olympus SZX16 stereo microscope. The surface area was quantified using Image J (National Institutes of Health, Bethesda, MD, USA) and normalized against day 0 controls, in which all constructs measured 5 mm in diameter, regardless of group.

2.11 | Gene expression analysis of MSC-seeded hydrogels

On days 7, 21 and 42, total RNA was collected from constructs by sequential use of Trizol (Thermo Fisher Scientific) and RNeasy mini kit plus (Qiagen, Valencia, CA, USA), according to the manufacturers' instructions. Total RNA (500 ng) was reverse transcribed into cDNA using the SuperScript III first-strand synthesis kit (Thermo Fisher Scientific). Quantitative real-time polymerase chain reaction (PCR) was performed using SYBR® Green master mix (Applied Biosystems, Foster City, CA, USA) on a StepOnePlus real-time PCR system (Applied Biosystems). Relative expression of each target was calculated using the $\Delta\Delta C_T$ method with the arithmetic average of GAPDH and r18S expression used as the endogenous reference. Expression levels were normalized against day 7 GelMA samples. Primer sequences were as follows: GAPDH (forward: CAAGGCTGAGAACGGGAAGC; reverse: AGGGGGCAGAGATGATGACC); 18S (forward: GTAACCCGTTGAACCCCATT; reverse: CCATCCAATCGGTAGTAGCG), Sox9 (forward: CTGAGCAGCGACGTCATCTC; reverse: GTTGGGCGGCAGGTACTG), aggrecan (Acan; forward: GCTACACTGGCGAGCACTGTAACAT; reverse: GCGCCAGTTCTCAAATTGCATGGC), collagen type II (Col2; forward: GGATGGCTGCACGAAACATACCGG; reverse: CAAGAAGCAGACCGGCCCTATG), and collagen type I (Col1; forward: TAAAGGGTCACCGTGGCT; reverse: CGAACCACATTGGCATCA).

2.12 | Biochemical composition of MSC-seeded hydrogels

On days 21 and 42, constructs were collected, dried and weighed. Following overnight digestion in papain, the sGAG and dsDNA content of each construct was determined, as described above in section 2.3. Relative sGAG production was calculated by dividing the total sGAG content by the total dsDNA content in each construct.

2.13 | Histology of MSC-seeded hydrogels

Histological sections were prepared on days 21 and 42 following a similar protocol as performed when characterizing the appearance of native and decellularized tendon and cartilage tissues described in section 2.2. Following rehydration, samples were stained with Safranin O/Fast Green (Electron Microscopy Sciences, Hatfield, PA, USA); nuclei were counterstained with haematoxylin. For immunohistochemical staining of collagen type II, antigen retrieval was achieved by incubation of slides for 30 min at 37 °C in chondroitinase ABC (100 mU/ml, Sigma) and hyaluronidase (250 U/ml, Sigma) suspended in 0.02% bovine serum albumin. Endogenous peroxidases were blocked with 3% H_2O_2 (in methanol). Non-specific binding was blocked with 1% horse serum. Samples were then exposed to rabbit anti-human collagen II primary antibody (ab34712, Abcam, Cambridge, MA, USA) diluted 1:400 in 1% horse serum overnight at 4 °C. Equine biotinylated secondary antibody binding, signal amplification and visualization were achieved through the use of VectaStain Universal Elite ABC Kit (Vector Laboratories, Burlingame, CA, USA) in accordance with the manufacturer's instructions. Nuclei were counterstained with haematoxylin QS (Vector).

2.14 | Statistical analysis

For quantitative assays, a minimum of six biological replicates were used for analyses. Data are presented as mean ± standard deviation. When comparing across multiple time points for a given hydrogel group, or among hydrogel groups for a given time point, one-way ANOVA with Tukey's post-hoc comparisons was performed. The comparison between two groups utilized Student's t-test. Results are noted as $p < 0.05$ (significant) or $p < 0.001$ (highly significant).

3 | RESULTS

3.1 | Characterization of decellularized tendon and cartilage ECM

The decellularization process successfully removed cellular content from tendon and cartilage tissues, as shown by the absence of nuclei on both H&E- and DAPI-stained sections (Figure 1a–h). Quantification of dsDNA content (Figure 1i) confirmed the removal of cellular content in both tendon (native vs. decellularized: 1131.1 ± 124.9 vs. 10.1 ± 4.9 ng/mg, $p < 0.001$) and cartilage (1281.9 ± 107.0 vs. 7.0 ± 1.0 ng/mg, $p < 0.001$). Total sGAG content (Figure 1j) was relatively low in both

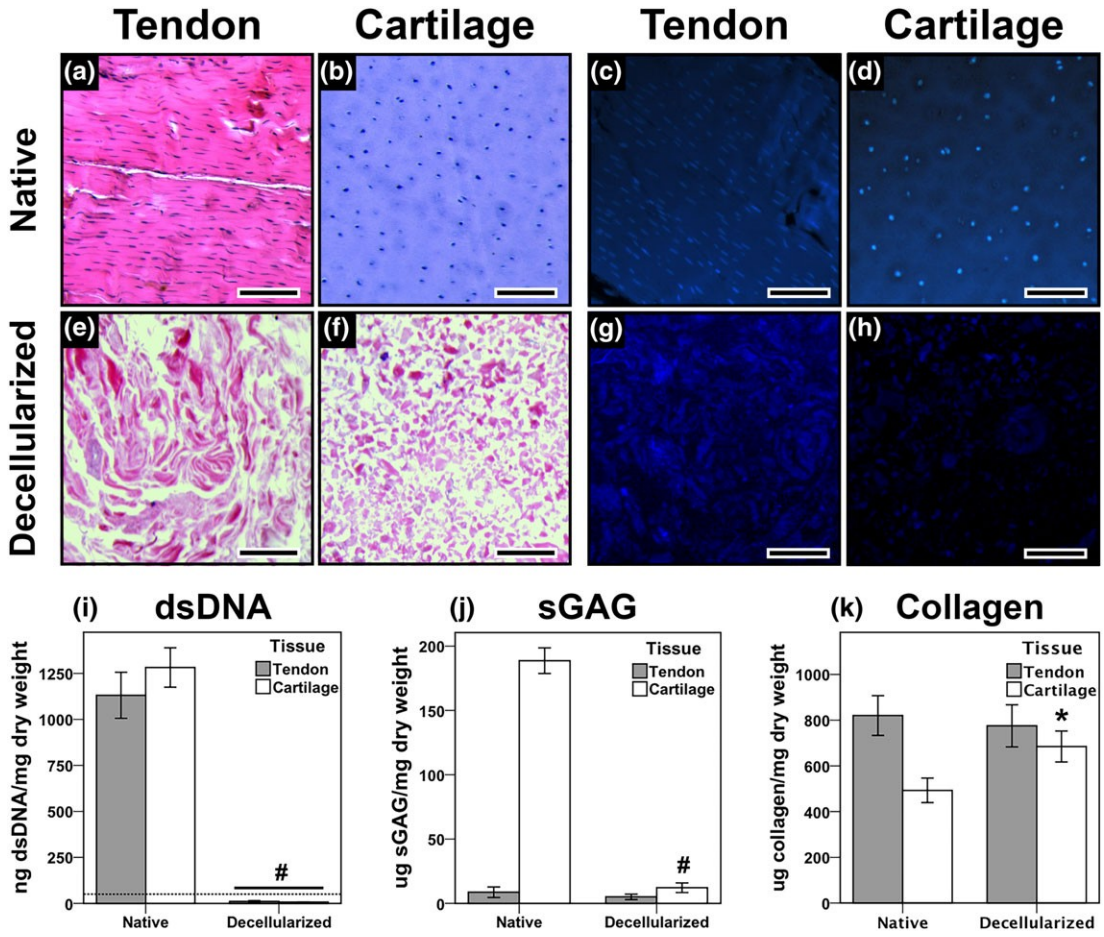

FIGURE 1 Characterization of decellularized tendon and cartilage extracellular matrix. Haematoxylin and eosin (H&E) staining (a, b) and 4',6-diamidino-2-phenylindole (DAPI) staining (c,d) of native tendon and cartilage, respectively. H&E staining (e,f) and DAPI staining (g,h) of decellularized tendon and cartilage. Double-stranded DNA content (i), sulfated glycosaminoglycan (j) and total collagen (k), normalized to dry weight of tissue for native and decellularized tissues. *p < 0.05; #p < 0.001, when comparing native with decellularized. n ≥ 6 for each tissue type

native and decellularized tendon ECM (8.7 ± 4.1 vs. 5.1 ± 2.1 μg/mg), but significantly reduced following decellularization of cartilage ECM (188.6 ± 10.0 vs. 12.2 ± 3.7 μg/mg, p < 0.001). Cartilage ECM (native vs. decellularized: 492.9 ± 53.7 vs. 684.8 ± 67.5 μg/mg, p < 0.05) showed a corresponding increase in total collagen, while remaining equivalent in native and decellularized tendon (Figure 1k).

3.2 | DOF

In the sample of CartilageMA, whose NMR spectrum is shown in Figure 2, there was the simultaneous presence of vinyl protons of both the methacrylate bound to collagen (peak #1) and the free methacrylic acid (peak #2), probably due to inefficient (or not proper) dialysis. The preliminary assignment of the free methacrylic acid resonances and those of bound methacrylate were obtained using chemical shift and peak-broadening considerations, corroborated by ^{1}H-^{13}C HSQC and unambiguously confirmed by spiking the sample with authentic material. The theoretical collagen sequence was inferred from the Protein Knowledgebase (free data base) and the composition in amino acids was calculated, using the ProtParam tool (ExPASy Server, bio-information resources portal), as follows: phenylalanine 1.7%, tyrosine 3.0%, tryptophan 0.5%. Each amino acid contributes to the total integrated intensity of aromatic signals (the spectrum region between 6.8 and 7.7 ppm, in Figure 2), with a different number of resonances and in a different proportion according to the amino acid composition. Particularly, the phenylalanine contributes with five resonances to the 32.7% of the aromatic signal intensity [(1.7/5.2) × 100], hence for 1.64, similarly, the tyrosine with four resonances to the 57.7% of signals, thus for 2.31, whereas the tryptophan contribution is 9.62% (five resonances), hence for only 0.48. The sum of all contributions, 4.43, features the normalization factor for resonance number. Experimentally, the integrated intensity of aromatic signals, calibrated at 100, has returned a relative value of 187.06 for the integrated intensity the vinyl methacrylate peak at 5.73 ppm. After normalization for resonance number factor, previously accounted (4.43), the integrated intensity of aromatic signals returns the value of 22.57 (100/4.43), therefore the integrated intensity of the methacrylate peak is 8.29 times more intense than that of aromatic signals (187.06/22.57). As the aromatic amino acids are 5.2% of all amino acids in the collagen, proportionally, the methacrylate will be 43.1% (8.28 × 5.2%). This value was assumed as the DOF.

Analogously, in the GelMA spectrum (spectrum not reported) a certain amount of free methacrylic acid together with the vinyl methacrylate peaks bound to the polymer was observed. The DOF of

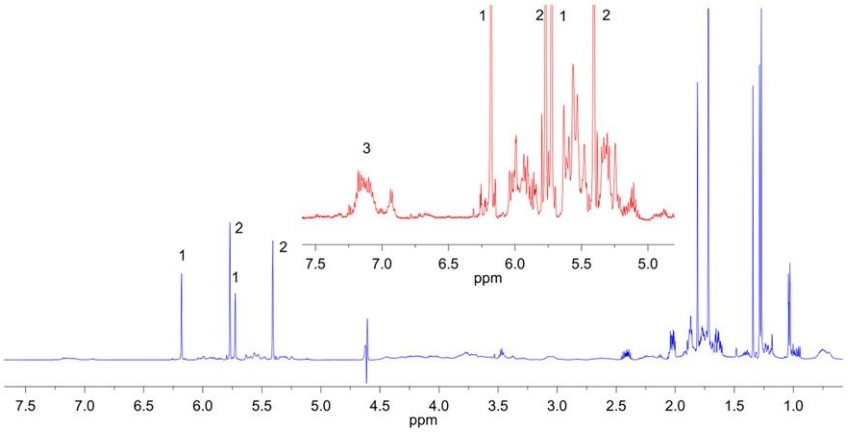

FIGURE 2 (1D)-NOESY presat. Nuclear magnetic resonance (NMR) spectrum of methacrylated cartilage recorded in D_2O/DCl 0.1 M. The inset shows the expanded region between 5 and 7.5 ppm that includes the signals of free methacrylic acid (peak #2), the methacrylate bound to the collagen (peak #1) and the aromatic collagen residues (peak #3). The degree of functionalization was estimated from the ratio between the integrated intensities of aromatic collagen signals (#3) and the integrated intensity of a methacrylate peak (#1), each normalized to their proton numbers

GelMA was calculated according to Brinkman, Nagapudi, Thomas, et al. (2003) as the ratio between the integrated area of a methacrylate peak and the integrated peaks area between 7.1 and 7.3 ppm. The value obtained was approximately 40%, similar to that of CartilageMA.

3.3 | Gross confirmation of thermoresponsiveness, photoresponsiveness

Preceding exposure to ultaviolet light,all ECM-derived hydrogels were liquid at 4 °C, whereas GelMA was transiently gelled (Figure 3a, top left). Upon exposure to UV light, only methacrylated hydrogels (GelMA, TendonMA, CartilageMA) underwent irreversible gelation (Figure 3a, bottom left). Conversely,if hydrogels were incubated for 1 h at 37 °C in the absence of light, the ECM-derived constructs showed thermoresponsive gelation whereas GelMA returned to a liquid state (Figure 3a, top right). Although the methacrylated hydrogels (TendonMA, CartilageMA) underwent temperature-mediated self-polymerization, the resulting hydrogels shrank in comparison with their non-methacrylated counterparts, suggesting a compromised thermoresponsiveness due to the process of methacrylation. Following incubation at 37 °C with subsequent UV light exposure, all hydrogels were irreversibly gelled (Figure 3a, bottom right).

3.4 | Surface ultrastructure

Only gelled hydrogels could be examined by SEM. Additionally, TendonMA and CartilageMA scaffolds that underwent thermal

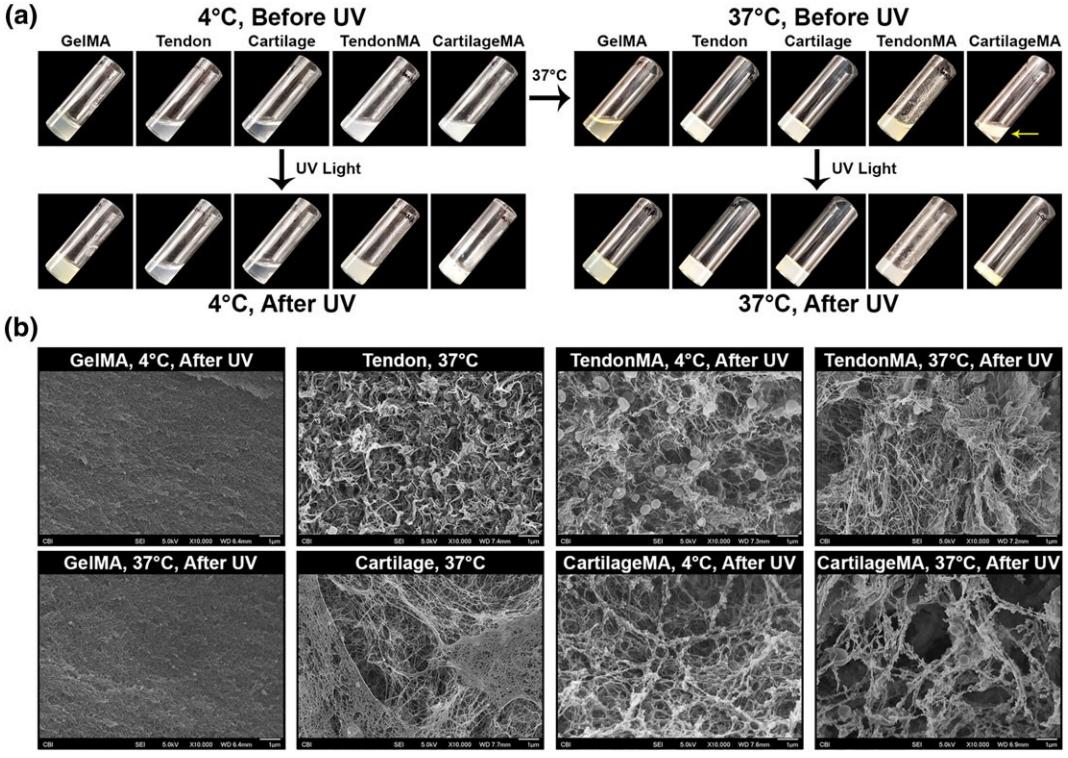

FIGURE 3 Characterization of hydrogel structure. Gross images demonstrating gelation due to temperature-mediated self-polymerization and/or photocrosslinking upon exposure to ultraviolet light (a).Methacrylated extracellular matrix hydrogels that underwent thermal gelation (preceding ultraviolet light exposure) frequently shrank (a; top right, yellow arrow). Surface ultrastructure of hydrogels as determined by scanning electron microscopy (b). Magnification = 10 000×; scale bar = 1 μm

gelation alone (no UV exposure,Figure 3b, top right) possessed weak mechanical integrity and were not maintained during critical point drying. GelMA hydrogels, regardless of temperature, exhibited a rough but relatively flat surface morphology at high magnification (10 000×, Figure 3b). Conversely, thermally induced non-methacrylated hydrogels (tendon, cartilage) exhibited a nanofibrous network. A similar nanofibrous architecture was seen in photocrosslinked TendonMA and CartilageMA preceding thermal induction, although globular structures were increasingly seen lining the fibrils. With thermoinduction and subsequent UV exposure, TendonMA and CartilageMA demonstrated a similar fibrillar structure, yet tended to have greater condensation of fibrils with a corresponding increase in pore size.

3.5 | Cell-mediated contraction of hydrogels

Non-methacrylated hydrogels experienced rapid cell-mediated contraction, with tendon and cartilage hydrogels measuring 16% and 18% of initial area on day 7 (Figure 4). Although cartilage constructs continued to slowly contract through day 42, tendon hydrogels demonstrated a small increase in area,resulting in a significant difference between the non-methacrylated hydrogels beginning on day 14. By contrast, methacrylated hydrogels maintained a larger surface area over the culture period. TendonMA constructs maintained the initial area size until day 14, experiencing a gradual decline thereafter. On the other hand, CartilageMA constructs contracted more quickly, reaching a relative area of 61% of day 14, at which time hydrogel disintegration could be grossly appreciated. As compared with day 14, CartilageMA area increased on days 21 and 42, but this change in size was at least partially attributable to loss of mechanical integrity. As expected, GelMA hydrogels minimally contracted over 6 weeks (Figure 4). Similarly, all acellular hydrogels showed minimal change in area over 6 weeks (Figure S1).

3.6 | Gene expression analysis of MSC-seeded constructs

As a control, GelMA hydrogels demonstrated stable expression of chondrogenic transcription factor, Sox9, at the three measured time points: days 7, 21, 42 (Figure 5a). By contrast, both Acan and Col2 expression increased from day 7 to day 42, whereas Col1 expression declined, an expression pattern indicative of a more hyaline cartilage phenotype. Non-methacrylated ECM hydrogels demonstrated a similar expression pattern with regards to Sox9, Acan and Col2, albeit delayed and/or diminished in magnitude. Of interest, tendon constructs more closely paralleled the relative expression pattern of GelMA constructs, whereas cartilage constructs demonstrated significantly lower levels of Sox9, Acan and Col2 expression by day 42. Furthermore, both non-methacrylated ECM hydrogels showed higher Col1 expression at every time point in comparison with GelMA constructs, indicative of greater fibrochondrogenic differentiation. Although TendonMA constructs showed an expression pattern similar to their non-methacrylated counterpart, CartilageMA constructs did not support robust expression of ECM proteins over the culture period, presumably due to the compromised integrity of these hydrogels as noted earlier (Figure 4). Similarly, all acellular hydrogels showed minimal change in area over 6 weeks (Figure S1).

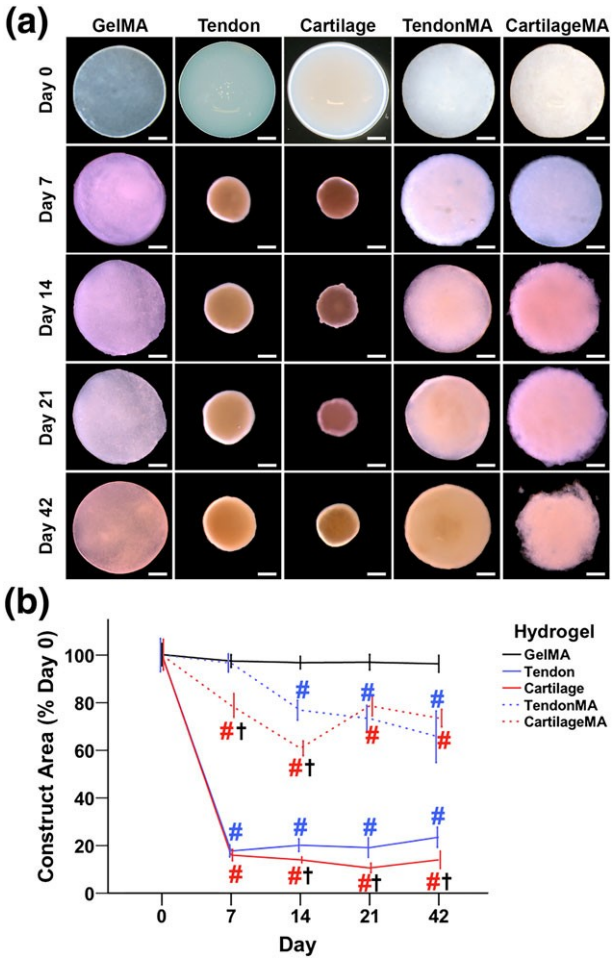

FIGURE 4 Cell-mediated contraction of hydrogels. Gross images of hydrogels over 42 days of culture in full chondrogenic medium (a); scale bar = 1 mm. Quantification of construct area normalized against day 0 constructs (5 mm diameter) (b). #$p < 0.001$as significant reduction in area compared with day 0. †$p < 0.001$ as significant difference between tendon and cartilage hydrogels of same functional group (non-methacrylated or methacrylated)

3.7 | Biochemical composition of MSC-seeded constructs

As all constructs possessed the same initial cell density (20×10^6/ml), differences in dsDNA content among hydrogels on day 42 indicate cell proliferation, as negligible change in cellular content was found from day 0 to day 42 in GelMA (data not shown). Non-methacrylated hydrogels supported cell proliferation, with cartilage constructs supporting the highest cell content (Figure 5b). Conversely, methacrylated ECM hydrogels did not support significant increases in dsDNA cell number. Total sGAG content was highest in GelMA constructs (77.8 ± 5.5 μg/mg). Non-methacrylated tendon (65.0 ± 3.5 μg/mg) and cartilage (61.0 ± 9.9 μg/mg), although less than GelMA controls, possessed higher sGAG content than TendonMA (26.2 ± 6.4 μg/mg) and CartilageMA constructs (2.2 ± 0.8 μg). Likewise, normalized sGAG content was significantly lower in ECM hydrogels as compared against GelMA (Figure 5b).

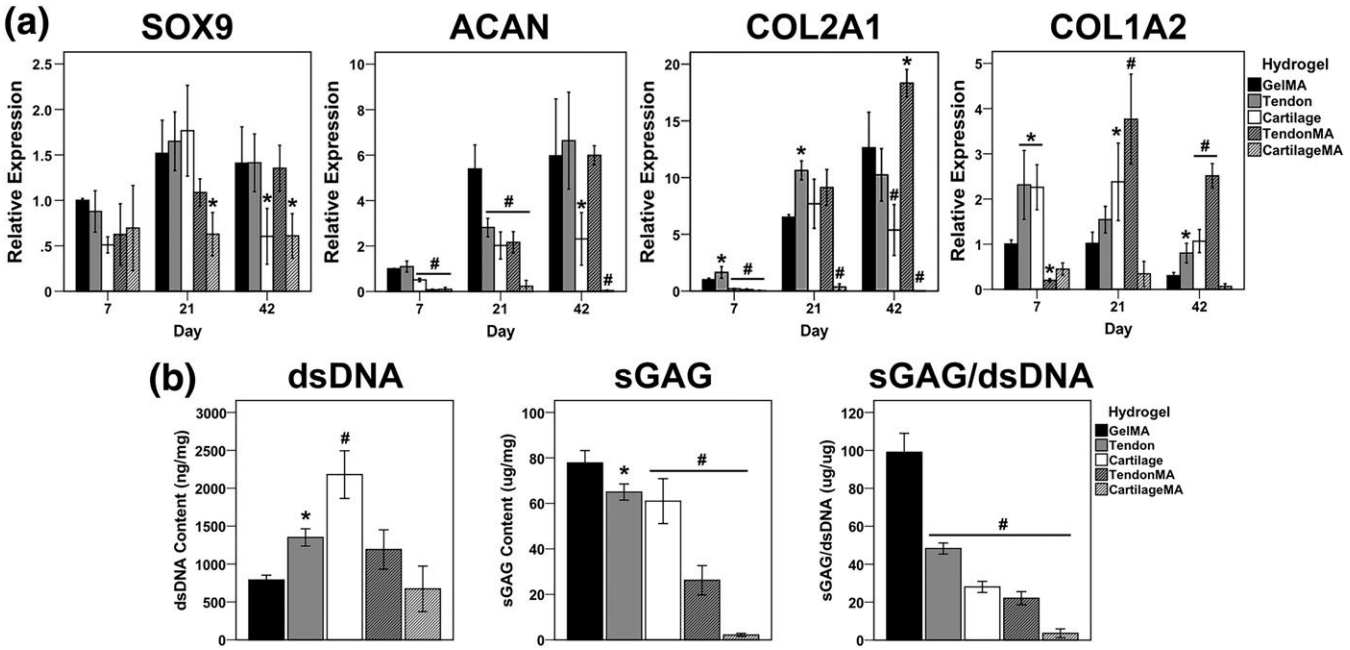

FIGURE 5 Gene expression and biochemical composition of constructs. Real time (RT)-PCR analysis for gene expression, with relative expression normalized to day 7 methacrylated gelatin (GelMA) constructs (a)*p < 0.05; #p < 0.001, as compared against GelMA of the same time point. (b) Biochemical composition of constructs on day 42. *p < 0.05; #p < 0.001, as compared against day 42 GelMA constructs

3.8 | Histology

Safranin O staining demonstrated increasing proteoglycan deposition in the GelMA constructs, with a gradient of decreasing intensity moving centrally from the periphery. Nevertheless, proteoglycan deposition could be discerned in the most inner regions of GelMA constructs on day 21, with greater and more homogenous distribution by day 42 (Figure 6a, f, k, p). Non-methacrylated ECM hydrogels, on the other hand, showed more heterogeneous staining intensity, with little qualitative difference when comparing tendon against cartilage hydrogels. By day 42, both tendon and cartilage constructs showed continued proteoglycan deposition. TendonMA constructs similarly showed heterogeneity in staining, but in a more pronounced manner. Namely, proteoglycan staining was distinctly localized to the perimeter of the hydrogel on day 21, suggesting limited diffusion of the TGF-β-supplemented medium into the interior region (Figure 6d, i). Nevertheless, by day 42, greater proteoglycan deposition was seen in the construct interior, but pronounced heterogeneity remained. By contrast, the CartilageMA constructs demonstrated negligible proteoglycan deposition (Figure 6e,j, o, t), in agreement with the assays for gene expression and biochemical composition (Figure 5). Rather, cell nuclei could be seen in varying regions of sparse and dense ECM, but equally suggestive of minimal neotissue formation.

Immunohistochemical staining of Col2 showed a similar pattern to Safranin O staining (Figure 7). Increasing Col2 staining, extending from the periphery inward, was seen in GelMA constructs at both time points (Figure 7a, p). Tendon and TendonMA showed increasing, but heterogeneous, staining intensity over time (Figure 7b, d, l, n). The non-methacrylated cartilage hydrogels exhibited regions of intense staining, presumably corresponding to the collagen type II of native cartilage tissue, with fainter regions probably indicating neotissue formation (Figure 7c, m). CartilageMA constructs similarly displayed dark staining indicative of the native cartilage tissue, with little deposition of new matrix (Figure 7e, o).

4 | DISCUSSION

In this study, hydrogels derived from decellularized cartilage and tendon were further functionalized with methacrylate groups, as confirmed by ^{1}H NMR spectroscopy. Although both non-methacrylated and methacrylated ECM hydrogels underwent thermoresponsive gelation, the latter demonstrated a compromised capacity, as similarly reported by Gaudet and Shreiber (2012) upon methacrylating collagen type I. Conversely, methacrylated hydrogels formed fine networks of collagen fibrils similar in appearance to their non-methacrylated counterparts, although further characterization of the network architecture was not performed. Methacrylation successfully slowed cell-mediated contraction, with methacrylated hydrogels at 6 weeks measuring approximately 70% of the initial area, whereas non-methacrylated hydrogels measured less than 20% of the initial area. These results agree with a recent study by Beck et al. (2016) in which methacrylate groups were added to a pepsin-soluble devitalized cartilage paste. Despite an improved maintenance of initial construct size, the methacrylation process compromised the long-term stability of CartilageMA constructs, which demonstrated fibrillation and subsequent disintegration beginning at day 14 and extending through to day 42. Why CartilageMA constructs experienced greater instability than TendonMA constructs is unclear, but is probably attributable to differences in the biochemical composition of these two tissues.

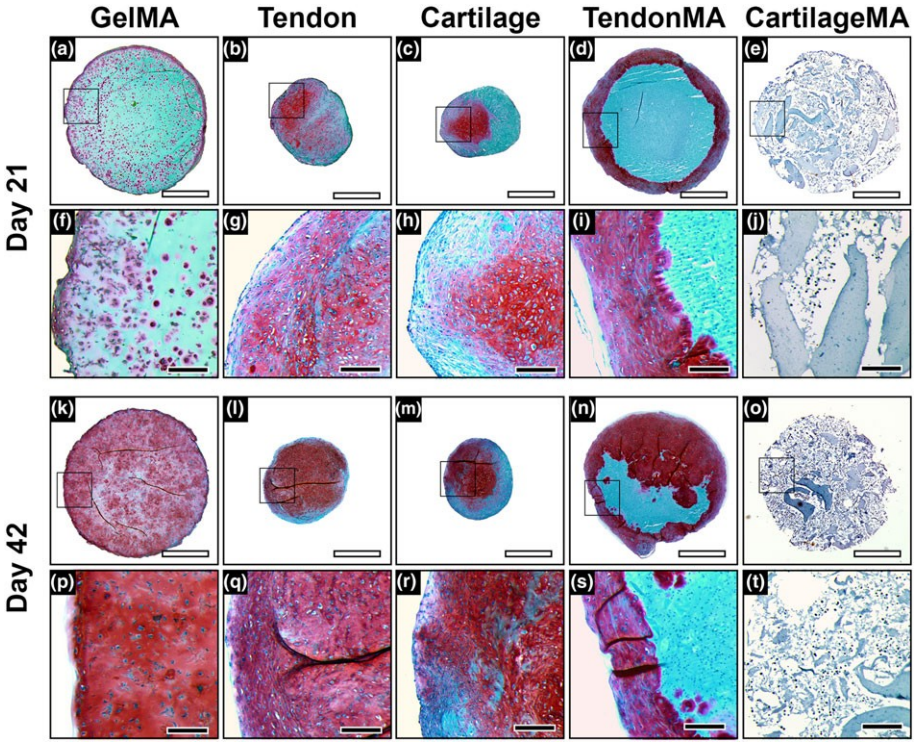

FIGURE 6 Safranin O staining. Low magnification on day 21 (a–e) and day 42 (k–o); scale bar = 1 mm. High magnification on day 21 (f–j) and day 42 (p–t); scale bar = 200 μm

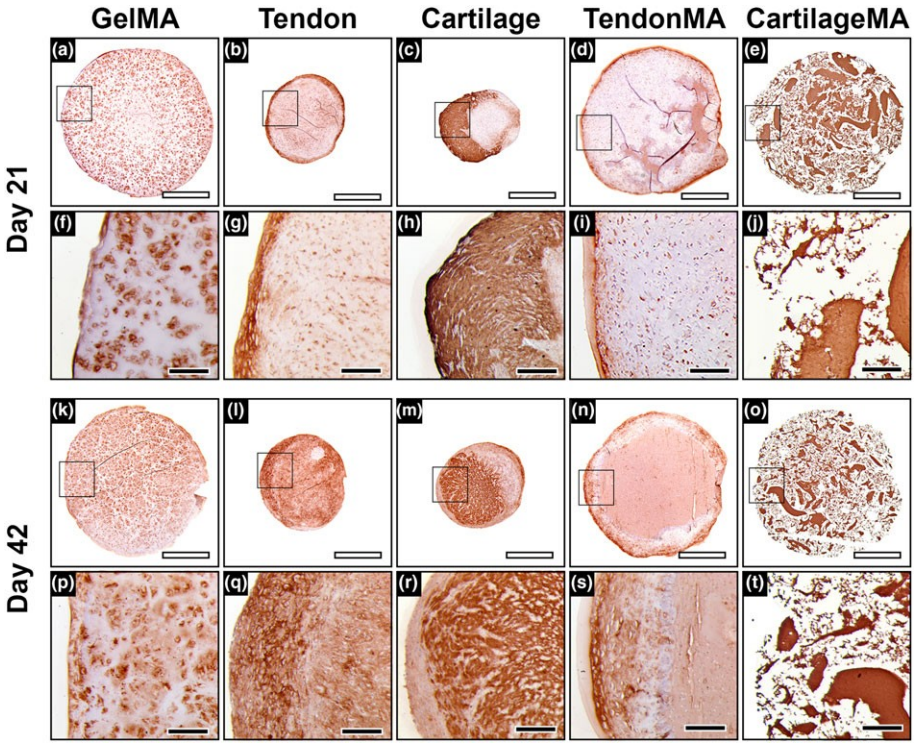

FIGURE 7 Collagen type II immunohistochemical staining. Low magnification on day 21 (a–e) and day 42 (k–o); scale bar = 1 mm. High magnification on day 21 (f–j) and day 42 (p–t); scale bar = 200 μm

Hydrogel integrity was essential for chondrogenic differentiation and matrix deposition by encapsulated MSCs, as demonstrated by the inferiority of the CartilageMA constructs when measuring gene expression, biochemical composition and histology. By contrast, TendonMA constructs demonstrated a similar gene expression pattern to non-methacrylated tendon constructs, but reduced sGAG content and greater heterogeneity in histological staining intensity. In particular, proteoglycan- and collagen type II-rich regions were found principally at the periphery of TendonMA constructs, suggesting limited diffusion of the TGF-β3-supplemented medium. In totality, the inferiority of

methacrylated hydrogels in supporting chondrogenic differentiation is in agreement with related studies. Namely, the Guilak group demonstrated reduced chondroinductivity in scaffolds engineered from cartilage ECM when increasing the crosslinking density by chemical or physical methods (Cheng, et al., 2013; Rowland et al., 2013). Similarly, Vickers, Squitieri, and Spector (2006) found that an increasing crosslink density reduced chondrogenic differentiation of chondrocytes seeded in a collagen type II-GAG scaffold. Although the independent chondroinductivity of methacrylated cartilage, tendon and meniscus was not explored by Visser Levett, et al. (2015), the inclusion of these methacrylated ECM hydrogels within GelMA hydrogels (2% ECM, 8% GelMA) did not enhance chondrogenic differentiation. Taken together, these data confirm that alterations in cell-matrix interactions mediated by the introduction of non-physiological crosslinks (e.g. methacrylate groups, dihydrothermal, genipin) can compromise the inherent bioactivity of native ECM proteins.

On the other hand, the inherent chondroinductivity of pepsin-solubilized ECM hydrogels is relatively unknown. As compared with collagen type I hydrogels, solubilized decellularized cartilage ECM was reported to upregulate Sox9 and Col2α1 expression by only a modest 1.5-fold increase (Pati et al., 2014). Similarly, Rutgers et al. (2013) found no difference between hydrogels of collagen type I or collagen type II, respectively, the principal structural proteins of tendon and cartilage, in terms of promoting chondrogenesis. In this study, non-methacrylated cartilage hydrogels did not enhance chondrogenic gene expression or matrix deposition, as compared against non-methacrylated tendon hydrogels or GelMA. By contrast, the inclusion of pulverized cartilage-derived matrix particles within hydrogels (Almeida et al., 2016; Visser, Gawlitta, et al., 2015) or as molded scaffolds (Rowland, Colucci, & Guilak, 2016; Rowland et al., 2013) has been shown to robustly upregulate chondrogenesis of seeded cells. Similarly, our recent work (Yang et al., 2013) and that of others (Zhang et al., 2009) has found that a urea-soluble (i.e. non-collagenous) fraction of the ECM can promote tissue-specific differentiation when added to defined polymeric hydrogels such as collagen or GelMA. These findings, in combination with the results of this study, suggest that pepsin-solubilized cartilage and tendon hydrogels, with a propensity for rapid cell-mediated contraction and negligible enhancement of chondrogenesis, may offer limited advantage as biomaterials for cartilage tissue engineering.

However, the possible utility of decellularized ECM as a biomaterial extends beyond homologous cell differentiation. Rather, ECM scaffolds, through the release of matricryptic peptides, are capable of recruiting progenitor cells (Beattie, Gilbert, Guyot, et al., 2009) and modulating the inflammatory response in vivo (Sicari et al., 2014), often promoting a more favourable remodelling response than otherwise found with innate healing. Nevertheless, solubilized ECM from different tissues can exert distinct immunomodulatory effects (Meng, Sliyka, Dearth, & Badylak, 2015), reinforcing the importance of ultimately evaluating ECM-derived scaffolds in vivo. Furthermore, Keane et al. (2015) found that the in vitro tissue-specific bioactivity of homologous ECM matrices did not translate into improved healing in vivo, as compared against ECM scaffolds derived from non-homologous tissues. Therefore, hydrogels derived from decellularized tendon or cartilage may enhance a site-appropriate healing response despite demonstrating little benefit in promoting homologous cell differentiation in vitro. As support, Kim et al. (2014) reported enhanced healing in a rat Achilles tendon defect model after injecting a tendon ECM hydrogel. However, the benefit of using the tendon ECM-derived hydrogel, as opposed to a purified collagen hydrogel, was not explored.

In addition to the absence of in vivo experiments, there were several limitations in this study. Cell-mediated contraction of non-methacrylated hydrogels produced spherically shaped constructs, limiting the accurate assessment of compressive mechanical properties. Similarly, the compromised thermoresponsiveness of methacrylated ECM hydrogels complicated the characterization of rheological properties. Further optimization of these assays would provide a more complete characterization of the fabricated hydrogels. However, as the principal aim of this study was to evaluate the chondroinductive capacity of homologous (i.e. cartilage) and non-homologous (i.e. tendon) hydrogels, these incomplete data were excluded from the final analysis. As noted previously, the compromised thermoresponsiveness of methacrylated ECM hydrogels also prevented imaging (by SEM) of their surface ultrastructure before UV exposure, as these hydrogels did not survive the preceding step of critical point drying. Furthermore, it is likely that the ultrastructure of the native gelated hydrogels was altered by the glutaraldehyde fixation step before SEM imaging. Analyses of gene expression and protein deposition of additional chondrogenic (or tenogenic) transcription factors and matrix proteins could have been performed through PCR and immunohistochemistry, respectively. Given the intended application of the hydrogels in cartilage tissue engineering, and in accordance with related publications, the included targets were considered the most relevant.

Finally, the chondrogenicity of all ECM hydrogels was compared against GelMA as a control. As GelMA fails to form a stable hydrogel at concentrations less than 4% (w/v), whereas decellularized tendon and cartilage ECM is insufficiently solubilized by pepsin at concentrations above 3% (w/v), comparisons of all hydrogels at the same protein concentration could not be performed. Additionally, it is noteworthy that as GelMA hydrogels have been well characterized and shown to be a suitable biomaterial for cartilage tissue engineering, direct comparison against native hyaline cartilage as a gold standard was not performed, a needed control group that is seldom included in other related studies.

In conclusion, functionalization of pepsin-soluble hydrogels derived from decellularized cartilage and tendon ECM reduced cell-mediated contraction but compromised chondroinductivity. As compared with GelMA, ECM hydrogels did not enhance MSC chondrogenesis, nor were cartilage gels superior to tendon gels. Based on these findings and recent work using pulverized cartilage matrix or a urea-extracted soluble fraction, future work will explore the combination of these cartilage-derived components with GelMA hydrogels to engineer robust MSC-based constructs that mimic the cellular phenotype, biochemical composition and mechanical properties of native cartilage.

ACKNOWLEDGEMENTS

The authors thank Dr Jian Tan for MSC isolation and characterization. Benjamin B. Rothrauff is a pre-doctoral trainee supported by an NIH Training Grant (5T32 EB001026).

CONFLICT OF INTEREST

The authors have declared that there is no conflict of interest.

REFERENCES

Almeida, H. V., Eswaramoorthy, R., Cunniffe, G. M., Buckley, C. T., O'Brien, F. J., & Kelly, F. J. (2016). Fibrin hydrogels functionalized with cartilage extracellular matrix and incorporating freshly isolated stromal cells as an injectable for cartilage regeneration. Acta Biomaterialia, 36, 55–62.

Beattie, A. J., Gilbert, T. W., Guyot, J. P., Yates, A. J., & Badylak, S. F. (2009). Chemoattraction of progenitor cells by remodeling extracellular matrix scaffolds. Tissue Engineering Part A, 15, 1119–1125.

Beck, E. C., Barragan, M., Tadros, M. H., Kiyotake, E. A., Acosta, F. M., Kieweg, S. L., & Detamore, M. S. (2016). Chondroinductive hydrogel pastes composed of naturally derived devitalized cartilage. Annals of Biomedical Engineering, 44, 1863–1880.

Brinkman, W. T., Nagapudi, K., Thomas, B. S., & Chaikof, E. L. (2003). Photo-cross-linking of type I collagen gels in the presence of smooth muscle cells: mechanical properties, cell viability, and function. Biomacromolecules, 4, 890–895.

Cheng, N. C., Estes, B. T., Young, T. H., & Guilak, F. (2013). Genipin-crosslinked cartilage-derived matrix as a scaffold for human adipose-derived stem cell chondrogenesis. Tissue Engineering Part A, 19, 484–496.

Crapo, P. M., Gilbert, T. W., & Badylak, S. F. (2011). An overview of tissue and whole organ decellularization processes. Biomaterials, 32, 3233–3243.

Farnebo, S., Woon, C. Y. L., Schmitt, T., Joubert, L. M., Kim, M., Pham, H., & Chang, J. (2014). Design and characterization of an injectable tendon hydrogel: a novel scaffold for guided tissue regeneration in the musculoskeletal system. Tissue Engineering Part A, 20, 1550–1561.

Gaudet, I. D., & Shreiber, D. I. (2012). Characterization of methacrylated type-I collagen as a dynamic, photoactive hydrogel. Biointerphases, 7, 25.

Keane, T. J., DeWard, A., Londono, R., Saldin, L. T., Castleton, A. A., Carey, L., … Badylak, S. F. (2015). Tissue-specific effects of esophageal extracellular matrix. Tissue Engineering Part A, 21, 2293–2300.

Kim, M. Y., Farnebo, S., Woon, C. Y. L., Schmitt, T., Pham, H., & Chang, J. (2014). Augmentation of tendon healing with an injectable tendon hydrogel in a rat Achilles tendon model. Plastic and Reconstructive Surgery, 133, 645E–653E.

Lin, H., Yang, G., Tan, J., & Tuan, R. S. (2012). Influence of decellularized matrix derived from human mesenchymal stem cells on their proliferation, migration and multi-lineage differentiation potential. Biomaterials, 33, 4480–4489.

Lin, H., Cheng, A. W.-M., Alexander, P. G., Beck, A. M., & Tuan, R. S. (2014). Cartilage tissue engineering application of injectable gelatin hydrogel with in situ visible-light-activated gelation capability in both air and aqueous solution. Tissue Engineering Part A, 20, 2402–2411.

Lomas, A. J., Ryan, C. N. M., Sorushanova, A., Shologu, N., Sideri, A. I., Tsioli, V., … Zeugolis, D. I. (2015). The past, present and future in scaffold-based tendon treatments. Advanced Drug Delivery Reviews, 84, 257–277.

Makris, E. A., Gomoll, A. H., Malizos, K. N., Hu, J. C., & Athanasiou, K. A. (2015). Repair and tissue engineering techniques for articular cartilage. Nature Reviews Rheumatology, 11, 21–34.

Meng, F. W., Slivka, P. F., Dearth, C. L., & Badylak, S. F. (2015). Solubilized extracellular matrix from brain and urinary bladder elicits distinct functional and phenotypic responses in macrophages. Biomaterials, 46, 131–140.

Ning, L. J., Zhang, Y. J., Zhang, Y., Qing, Q., Jiang, Y. L., Yang, J. L., … Qin, T. W. (2015). The utilization of decellularized tendon slices to provide an inductive microenvironment for the proliferation and tenogenic differentiation of stem cells. Biomaterials, 52, 539–550.

Pati, F., Jang, J., Ha, D. H., Won Kim, S., Rhie, J. W., Shim, J. H., … Cho, D. W. (2014). Printing three-dimensional tissue analogues with decellularized extracellular matrix bioink. Nature Communications, 5, 11.

Rowland, C. R., Colucci, L. A., & Guilak, F. (2016). Fabrication of anatomically-shaped cartilage constructs using decellularized cartilage-derived matrix scaffolds. Biomaterials, 91, 57–72.

Rowland, C. R., Lennon, D. P., Caplan, A. I., & Guilak, F. (2013). The effects of crosslinking of scaffolds engineered from cartilage ECM on the chondrogenic differentiation of MSCs. Biomaterials, 34, 5802–5812.

Rutgers, M., Saris, D. B., Vonk, L. A., van Rijen, M. H., Akrum, V., Langeveld, D., … Creemers, L. B. (2013). Effect of collagen type I or type II on chondrogenesis by cultured human articular chondrocytes. Tissue Engineering Part A, 19, 59–65.

Schwarz, S., Elsaesser, A. F., Koerber, L., Goldberg-Bockhorn, E., Seitz, A. M., Bermueller, C., … Rotter, N. (2015). Processed xenogenic cartilage as innovative biomatrix for cartilage tissue engineering: effects on chondrocyte differentiation and function. Journal of Tissue Engineering and Regenerative Medicine, 9, 239–251.

Schwarz, S., Koerber, L., Elsaesser, A. F., Goldberg-Bockhorn, E., Seitz, A. M., Durselen, L., … Rotter, N. (2012). Decellularized cartilage matrix as a novel biomatrix for cartilage tissue-engineering applications. Tissue Engineering Part A, 18, 2195–2209.

Sicari, B. M., Dziki, J. L., Siu, B. F., Medberry, C. J., Death, C. L., & Badylak, S. F. (2014). The promotion of a constructive macrophage phenotype by solubilized extracellular matrix. Biomaterials, 35, 8605–8612.

Stabile, K. J., Odom, D., Smith, T. L., Northam, C., Whitlock, PW, Smith, B. P., … Ferguson, C. M. (2010). An acellular, allograft-derived meniscus scaffold in an ovine model. Arthroscopy, 26, 936–948.

Sutherland, A. J., Converse, G. L., Hopkins, R. A., & Detamore, M. S. (2015). The bioactivity of cartilage extracellular matrix in articular cartilage regeneration. Advanced Healthcare Materials, 4, 29–39.

Vickers, S. M., Squitieri, L. S., & Spector, M. (2006). Effects of cross-linking type II collagen-GAG scaffolds on chondrogenesis in vitro: dynamic pore reduction promotes cartilage formation. Tissue Engineering, 12, 1345–1355.

Visser, J., Gawlitta, D., Benders, K. E. M., Toma, S. M., Pouran, B., van Weeren, P. R., … Malda, J. (2015). Endochondral bone formation in gelatin methacrylamide hydrogel with embedded cartilage-derived matrix particles. Biomaterials, 37, 174–182.

Visser, J., Levett, P. A., te Moller, N. C. R., Besems, J., Boere, K. W., van Rijen, M. H., … Malda, J. (2015). Crosslinkable hydrogels derived from cartilage, meniscus, and tendon tissue. Tissue Engineering Part A, 21, 1195–1206.

Wolf, M. T., Daly, K. A., Brennan-Pierce, E. P., Johnson, S. A., Carruthers, C. A., D'Amore, A., … Badylak, S. F. (2012). A hydrogel derived from decellularized dermal extracellular matrix. Biomaterials, 33, 7028–7038.

Wu, J., Ding, Q., Dutta, A., Wang, Y., Huang, Y. H., Weng, H., … Hong, Y. (2015). An injectable extracellular matrix derived hydrogel for meniscus repair and regeneration. Acta Biomaterialia, 16, 49–59.

Yang, G., Rothrauff, B. B., Lin, H., Gottardi, R., Alexander, P. G., & Tuan, R. S. (2013). Enhancement of tenogenic differentiation of human adipose

stem cells by tendon-derived extracellular matrix. Biomaterials, 34, 9295–9306.

Yin, Z., Chen, X., Zhu, T., Hu, J. J., Song, H. X., Shen, W. L., … Ouyang, H. W. (2013). The effect of decellularized matrices on human tendon stem/progenitor cell differentiation and tendon repair. Acta Biomaterialia, 9, 9317–9329.

Zhang, Y. Y., He, Y. J., Bharadwaj, S., Hammam, N., Carnagey, K., Myers, R., … Van Dyke, M. (2009). Tissue-specific extracellular matrix coatings for the promotion of cell proliferation and maintenance of cell phenotype. Biomaterials, 30, 4021–4028.